BASH: Biomechanical Animated Skinned Human for Visualization of Kinematics and Muscle Activity

R. Schleicher[1], M. Nitschke[1], J. Martschinke[2], M. Stamminger[2], B. M. Eskofier[1], J. Klucken[3] and A. D. Koelewijn[1]

[1]*Machine Learning and Data Analytics Lab, Department Artificial Intelligence in Biomedical Engineering (AIBE), Friedrich-Alexander-Universität Erlangen-Nürnberg (FAU), Germany*

[2]*Chair of Visual Computing, Department of Computer Science, Friedrich-Alexander-Universität Erlangen-Nürnberg (FAU), Germany*

[3]*Department of Molecular Neurology, University Hospital Erlangen, Friedrich-Alexander-Universität Erlangen-Nürnberg (FAU), Germany*

Keywords: Biomechanics, Surface Visualization, Animation, Statistical Human Model, Kinematics, Muscle Activity.

Abstract: Biomechanical analysis of human motion is applied in medicine, sports and product design. However, visualizations of biomechanical variables are still highly abstract and technical since the body is visualized with a skeleton and muscles are represented as lines. We propose a more intuitive and realistic visualization of kinematics and muscle activity to increase accessibility for non-experts like patients, athletes, or designers. To this end, the Biomechanical Animated Skinned Human (BASH) model is created and scaled to match the anthropometry defined by a musculoskeletal model in OpenSim file format. Motion is visualized with an accurate pose transformation of the BASH model using kinematic data as input. A statistical model contributes to a natural human appearance and realistic soft tissue deformations during the animation. Finally, muscle activity is highlighted on the model surface. The visualization pipeline is easily applicable since it requires only the musculoskeletal model, kinematics and muscle activation patterns as input. We demonstrate the capabilities for straight and curved running simulated with a full-body musculoskeletal model. We conclude that our visualization could be perceived as intuitive and better accessible for non-experts than conventional skeleton and line representations. However, this has to be confirmed in future usability and perception studies.

1 INTRODUCTION

The progress in biomechanics has brought vast opportunities to analyse human movement (Ezati et al., 2019). Biomechanical simulations enable a reconstruction of recorded motion or prediction of a novel movement (Ezati et al., 2019; Falisse et al., 2019; Lin and Pandy, 2017; Nitschke et al., 2020). Humans are represented with physics-based musculoskeletal models to calculate biomechanical variables such as joint angles, joint moments and muscle activation. As the methodology continues to develop, applications in medicine, sports and product design are emerging. Hence, multiple user groups besides biomechanical engineers will inspect and interpret biomechanical variables in future. For example, a visualization of Parkinson-specific motion might be exploited for modern patient education (Udow et al., 2018) or for visual feedback for gait retraining (Richards et al., 2018; Van den Noort et al., 2015). As alternative to video analysis in sports which is restricted to a capture volume and might not always be available, motion could be reconstructed from inertial sensor data using musculoskeletal simulation (Dorschky et al., 2019b) and later be visualized for analysis with a human model. This reconstruction has the additional advantages that internal variables, such as movement-related forces, could be analysed for injury prevention (Bencke et al., 2018; Vannatta and Kernozek, 2015). Although musculoskeletal simulations can support product design of, for example, prostheses (Fey et al., 2012; Koelewijn and van den Bogert, 2016) or shoes (Dorschky et al., 2019a), they lack a proper tool to communicate design decisions with non-experts. In order to inspect and interpret the simulated biomechanical variables, a visualization has to be intuitive and accessible for non-experts like patients, athletes, or designers.

1.1 Related Work

A wide variety of biomechanical simulation frameworks exists for modelling and analysis of musculoskeletal models. AnyBody (Damsgaard et al.,

Schleicher, R., Nitschke, M., Martschinke, J., Stamminger, M., Eskofier, B., Klucken, J. and Koelewijn, A.
BASH: Biomechanical Animated Skinned Human for Visualization of Kinematics and Muscle Activity.
DOI: 10.5220/0010210600250036
In *Proceedings of the 16th International Joint Conference on Computer Vision, Imaging and Computer Graphics Theory and Applications (VISIGRAPP 2021) - Volume 1: GRAPP*, pages 25-36
ISBN: 978-989-758-488-6

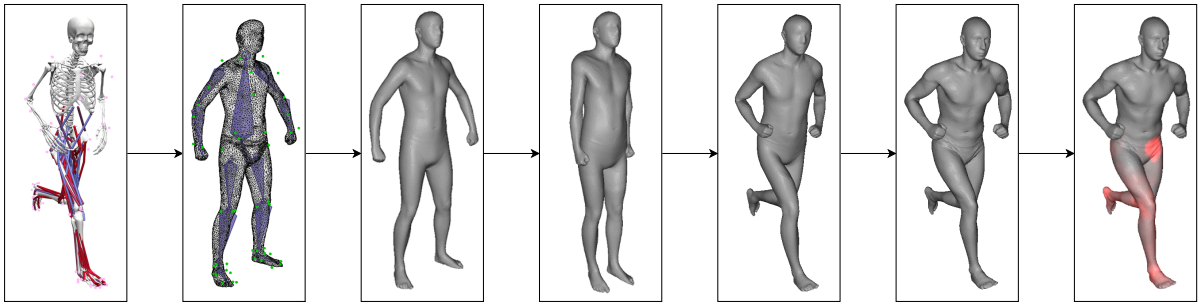

Figure 1: Proposed processing pipeline to visualize kinematics and muscle activity of biomechanical simulations using a skinned human model. From left to right it shows the musculoskeletal model visualized with OpenSim (Seth et al., 2018) and the proposed processing steps: creation of the BASH baseline model, scaling, initial pose matching, pose transformation, statistical deformation, and visualization of muscle activity.

2006), D-Flow (Geijtenbeek et al., 2011; Van den Bogert et al., 2013) and LifeModeler (McGuan, 2001) are commercial software packages and OpenSim (Delp et al., 2007; Seth et al., 2018) is an open-source software package. OpenSim is reaching a worldwide and rapidly growing community due to its accessibility (Seth et al., 2018) and its support for forward dynamics to predict novel movements. Abella and Demircan (2019) incorporated musculoskeletal models derived from OpenSim into the Unity environment to simultaneously track and analyse motion.

These software solutions focus on the simulation functionality and on an accurate representation of the modelled body segments and muscle tendon units (MTUs). Hence, they provide an interactive interface displaying bones only as simple geometric shapes and muscles as two-dimensional (2D) line representations (see for example the OpenSim visualization in Figure 1, left). Muscle activity is shown by color coding of the muscle pathways. Although these abstract and technical visualizations are well suited for users with biomechanical background, they are not appropriate for non-experts. The visualization of musculoskeletal simulations was integrated into a computer-aided design environment to facilitate user-centered design, but the model was still visualized with a skeleton and muscle pathways (Krüger and Wartzack, 2015).

Instead of using muscle pathways, muscles can be modelled with volumetric geometries to increase accuracy of the simulations or to study muscle deformation (Blemker and Delp, 2005; Maurice et al., 2009; Peeters and Pronost, 2014; Teran et al., 2003; Teran et al., 2005). However, volumetric muscle models are rarely used in biomechanical simulations since complexity of model creation and simulation increases considerably. Others include volumetric muscle models only for visualization of computed muscle activity to increase interpretability without using them for simulation (Pronost et al., 2011; Van den Bogert et al., 2013). Pronost et al. (2011) provided an OpenSim plugin with predefined muscle geometries that can be assigned to the MTUs of the musculoskeletal model. However, none of these visualizations for biomechanical analysis uses three-dimensional (3D) skinned human models. An overlay of volumetric muscle shapes on a video stream for color coding of muscle activity (Murai et al., 2010) might be closer to reality than the existing skeletal representations. This approach operates in real-time based on electromyography measurements. Nevertheless, it is not applicable if no video recording is available, which is the case when motion is reconstructed from inertial sensor data or when novel motions are predicted. Hence, 3D skinned human models might be the most intuitive visualization of reconstructed and predicted biomechanical movements especially for non-specialists.

In computer graphics, biomechanical and physical knowledge is also used to increase realism of human animations. Muscle and soft tissue deformation are modelled with mass-spring systems, finite element method, or finite volume method (Aubel and Thalmann, 2001; Lee et al., 2009; Lee et al., 2012; Murai et al., 2017; Sueda et al., 2008). Geometries have to be modelled by hand or based on medical image data and simulations often have high computational demands. Hence, these methods are usually only applied for single muscles or body parts. Alternatively, human surface models can be directly animated with data-driven methods without explicitly taking the deformation of underlying structures into account (Lee et al., 2012). An elegant way to create a virtual skin envelope is to use statistical parametric shape models, which are often used for animation of human subjects in motion (Cheng et al., 2018). Anguelov et al. (2005) first implemented a parametric model for pose-induced soft tissue deformation and body shape variation to perform Shape Completion and Animation of PEople (SCAPE). Parameters are learned from 3D full-body scans of various poses and people. They separate rigid (skele-

tal) and non-rigid deformations to simplify mathematically formulation and to accelerate the learning algorithm. However, the SCAPE model determines the soft tissue deformation based on only a static pose and does not take muscle activation or dynamics into account. The *Dyna* (Pons-Moll et al., 2015) model also reflects dynamic soft tissue deformations caused by motion. Nevertheless, the statistical surface models used in computer graphics lack the connection to traditional biomechanical simulations of musculoskeletal models. Torque-driven animation is intensively investigated to obtain authentic human motion instead of prescribing the motion (Geijtenbeek and Pronost, 2012; Jiang et al., 2019). But, in contrast to muscle control, torque control does not generate biologically reasonable motion since human torques are not limited to a constant range and the energy function minimizing torques does not reflect the human musculoskeletal system (Jiang et al., 2019).

1.2 Purpose

In this work, we aim to develop a method to animate 3D human surface models for biomechanical analysis. We propose the Biomechanical Animated Skinned Human (BASH) model which provides an animated skinned visualization of a musculoskeletal model defined in the commonly used OpenSim format (Seth et al., 2018) without requiring any additional data. The body proportions of the virtual human are automatically adapted to match the subject-specific dimensions of the musculoskeletal model. Kinematic coordinates are processed to apply pose transformation and thus to animate the skin envelope in order to reflect a movement. The statistical model SCAPE (Anguelov et al., 2005) should yield natural human appearance and realistic soft tissue deformations. Furthermore, muscle activity of underlying MTUs is highlighted on the surface which enables a kinetic analysis. We evaluate the pipeline with ten full-body musculoskeletal models scaled to each subject and simulated data of straight and curved running. Though this assumption has to be proven in further studies, we assume that our representation is more intuitive than conventional visualizations and therefore more accessible, especially for users without biomechanical background.

1.3 Outline

The processing pipeline is summarized in Figure 2. In Section 2, the biomechanical data and the SCAPE model are introduced. In Section 3, the generation of the baseline version of the proposed BASH model is described. Section 4 explains how the BASH model was matched to a subject-specific musculoskeletal model. Section 5 covers the animation and statistical deformation of the surface model. The visualization of muscle activity is presented in Section 6. The results of the experiments and analyses from Section 7 are evaluated and discussed in Section 8. The paper concludes with a short summary and outlook in Section 9. The code is publicly available at https://github.com/mad-lab-fau/BASH-Model.

2 VISUALIZATION INPUT

A musculoskeletal model, kinematics and muscle activity serve as biomechanical input for the visualization (see Figure 2). Since OpenSim (Seth et al., 2018) is a widely used open-source software for musculoskeletal simulations, its data format and framework is used. All variables belonging to the biomechanical data are denoted in this paper with a hat $\hat{\cdot}$. The musculoskeletal model consists of a skeletal structure where bone segments are connected via moving joints $\hat{\mathcal{J}} = \{\hat{J}_0, \ldots, \hat{J}_{N_{\hat{\mathcal{J}}}-1}\}$. Joints can be manipulated using generalized coordinates $\hat{\vec{q}}(t)$, thus defining the kinematics of the model over time t. Virtual markers $\hat{\mathcal{M}} = \{\hat{\vec{m}}_0, \ldots, \hat{\vec{m}}_{N_{\hat{\mathcal{M}}}-1}\}$ are commonly attached to the musculoskeletal model for subject-specific model scaling and inverse kinematics. Muscles are described by MTUs with 2D pathways $\hat{E}(t)$ and maximum isometric forces $\hat{f}_{max}$, among other parameters. Forces acting during a movement are encoded as muscle activation $\hat{a}(t)$ of a specific MTU.

To obtain a realistic surface representation of the musculoskeletal model, the human statistical SCAPE (Anguelov et al., 2005) model is used as basis. SCAPE, the first established method of its kind, provides a sophisticated framework for our approach. All variables belonging to the SCAPE model are denoted in this paper with a tilde $\tilde{\cdot}$. Training of pose parameters $\tilde{\mathbf{Q}}$ and shape parameters $\tilde{\mathbf{D}}$ was performed on full-body 3D scans from a large data set (Yang et al., 2014). Additionally, training of the shape coefficients was refined using further 3D scans (Hasler et al., 2009b; Hasler et al., 2009a; Hasler et al., 2010). In order to eliminate any pose deviations for the shape learning, a volume aware non-rigid mesh registration was performed (Colaianni et al., 2014). Training generates a template mesh $\tilde{\mathcal{V}}$ which corresponds to the envelope of a virtual person in static pose with average shape parameters.

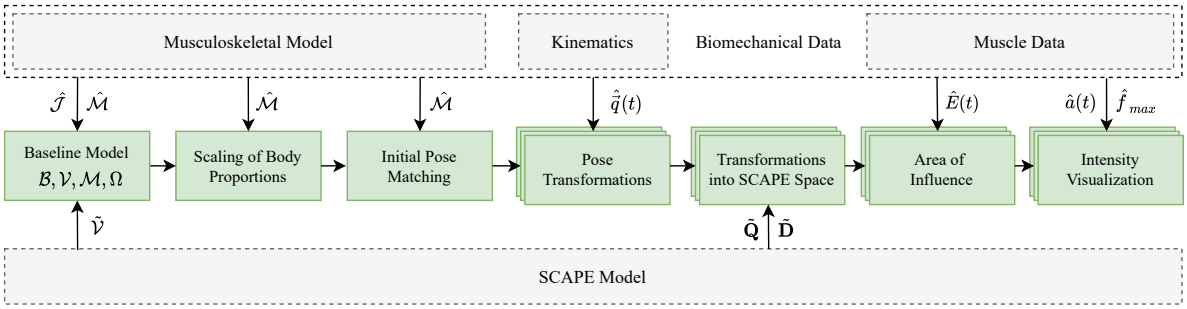

Figure 2: Processing pipeline to visualize kinematics and muscle activity using a skinned human surface model. The input of the pipeline (grey rectangles) and the processing steps (green rectangles) are explained in the following sections.

3 BASELINE MODEL

The simulated generalized coordinates of the musculoskeletal model cannot directly be applied to the SCAPE model due to differences in skeletal structures, body proportions and initial poses which would lead to an incorrect visualization. In particular, the disparate definition of the skeletal structure of both models is a challenge. The BASH model is developed to overcome the differences and to generate an accurate yet realistic 3D surface representation of the simulated musculoskeletal motion. Figure 3 illustrates the three components which define the BASH model:

- **Mesh geometry** to represent the model's surface and virtual appearance of the skinned human
- **Articulated skeleton** to enable surface deformations using the interconnected bones
- **Marker attachments** to create a clear relationship to the musculoskeletal model for scaling of body proportions and initial pose matching

The SCAPE template mesh $\tilde{\mathcal{V}}$ is used as the BASH geometry $\mathcal{V}$ with vertices $\vec{v}$. A skeletal armature with the same hierarchical composition as the musculoskeletal model is placed into the mesh by rigging the bones $\mathcal{B} = \{B_0, \ldots, B_{N_\mathcal{B}-1}\}$ as defined by the joints $\hat{\mathcal{J}}$ of the musculoskeletal model. Deviations in position and dimensions can be neglected since body proportions will be scaled in a separate step. Automatic computed skinning weights $\Omega_{\vec{v}} = \{\omega_{B_0}, \ldots, \omega_{B_{N_\Omega-1}}\}$ connect the skeleton and the mesh geometry (Kavan et al., 2009). The weight ω_B determines by how much the transformation of a bone B is transferred to its assigned vertices. The maximum number of influencing bones for one vertex is set to $N_\Omega = 4$ which is common in character animation due to efficiency in hardware (McLaughlin et al., 2011). Improperly assigned weights are corrected manually. Finally, virtual markers $\mathcal{M} = \{\vec{m}_0, \ldots, \vec{m}_{N_\mathcal{M}-1}\}$ corresponding to the markers $\hat{\mathcal{M}}$ of the musculoskeletal model are attached to the BASH model at landmark points near the surface to establish a relationship between the models. The markers are used to determine body proportions and to match the initial poses. The resulting generic version of the BASH model reflects a non-scaled musculoskeletal model with a specific anatomical structure.

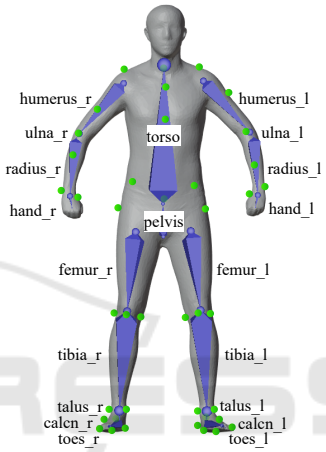

Figure 3: The conceptual design of the generic BASH model on the basis of SCAPE (Anguelov et al., 2005). It incorporates a surface mesh, an underlying articulated skeleton and attached marker points.

4 MODEL MATCHING

The baseline model has to be matched to a scaled version of the musculoskeletal model in its initial pose. This preprocessing step is performed once for a subject before animation.

4.1 Scaling of Body Proportions

In musculoskeletal modelling, individual variations in body proportions are taken into account by adjust-

ing the body segments using recorded marker positions (Delp et al., 2007). Using the same principle, we match the subject's anthropometry and ensure a realistic visualization by scaling segment sizes based on the defined virtual marker positions (see Figure 4). For each bone B, an uniform scaling transformation $\mathbf{S}_B$ is determined as average ratio between marker distances of the musculoskeletal model and of the generic BASH model.

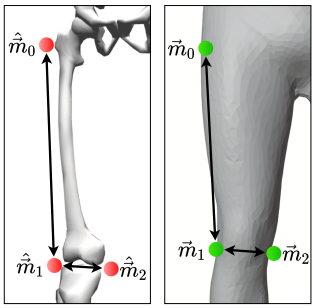

Figure 4: 3D positions of attached markers $\hat{\vec{m}}$ and $\vec{m}$ are used to scale body segments.

However, the scaling with matrix $\mathbf{S}_B$ is not applied directly in bone space since a change of bone size should only be applied to a particular bone B and not inherited through the skeletal hierarchy. Therefore, the new position $\mathbf{N}'_B$ of a bone B is computed by propagation through the skeleton starting at the root node:

$$\mathbf{N}'_B = \mathbf{N}'_{B_{parent}} \cdot \mathbf{N}_B \cdot \mathbf{S}_B \cdot \mathbf{S}^{-1}_{B_{parent}}, \quad (1)$$

where $\mathbf{N}_B$ is the 3D state of the bone before scaling. Scaling of the parent bone B_{parent} is reversed by multiplying the inverse scaling matrix $\mathbf{S}^{-1}_{B_{parent}}$ to avoid inheritance. For the root node, $\mathbf{N}'_{B_{parent}}$ and $\mathbf{S}^{-1}_{B_{parent}}$ are the identity matrix. To scale the generic mesh, the new position $\mathbf{N}'_B$ is multiplied by the inverse offset matrix ${}^{B}_{W}\mathbf{O}^{-1}$ which denotes the projection from bone space B to world space W. The resulting transformation matrices are applied to the markers and vertices of the generic mesh. Consequently, linear blend skinning shifts all vertices $\vec{v}$ by the extent of the defined skinning weights $\Omega_{\vec{v}}$ which simultaneously prevents hard borders and noticeable gaps between limbs (Magnenat-Thalmann et al., 1988).

4.2 Initial Pose Matching

Within OpenSim, pose transformations are specified by generalized coordinates. However, the relation between the initial pose of the musculoskeletal model and the scaled BASH model is unknown and has to be established before deploying any pose transformation. This relation is described by a change of basis, i.e. by a projection ${}^{\hat{f}}_{B}\mathbf{P}$ from the coordinate system of joint $\hat{f}$ of the musculoskeletal model to the corresponding coordinate system of bone B of the scaled BASH model. The generalized coordinates $\hat{\vec{q}}$ define the pose of the musculoskeletal model which matches the initial pose of the scaled BASH model. They are obtained by inverse kinematics using the OpenSim application programming interface (API) (version 4.0) (Seth et al., 2018). In inverse kinematics, the sum of squared distances between corresponding marker pairs of the two models is minimized. For the resulting pose, the projection matrix ${}^{\hat{f}}_{B}\mathbf{P}$ is received from the OpenSim API as global transformation of the bones with respect to the ground. Applying the inverse transformations to the scaled BASH model causes a deformation of the mesh via skinning weights to match the pose of the musculoskeletal model.

5 ANIMATION AND STATISTICAL DEFORMATION

In order to create an animation of the simulated musculoskeletal model, a series of transformations is applied to the scaled BASH model for each time frame t of the motion sequence.

5.1 Pose Transformations

Traditional character animation techniques are used to obtain an animated surface representation of the input kinematics. The affine transformation $\hat{\mathbf{T}}_{\hat{f}}(t)$ contains the translation and the rotation defined by the generalized coordinates $\vec{q}(t)$ given in the OpenSim motion file. For each frame, the input transformation $\hat{\mathbf{T}}_{\hat{f}}(t)$ can be directly applied to the bones of the scaled BASH model in the global coordinate system due to prior scaling and initial pose matching. The surface deformation was achieved by linear blend skinning with previously computed skinning weights. As a result, the pose transformed BASH model contained the aggregated animation based on the given movement of the musculoskeletal model.

5.2 Transformations into SCAPE Space

Statistical transformations introduced in the SCAPE model (Anguelov et al., 2005) are performed for each time frame t after the pose transformation to achieve realistic soft tissue deformations and therefore enhance the natural appearance. Before applying the statistical transformations, the rigid part rotations $\mathbf{R}_{\tilde{B}}$

of all body parts $\tilde{B}$ have to be determined in order to define the current pose in the SCAPE space. The original method proposed by Anguelov et al. (2005) is adapted to operate without a full body scan of the target person by using the pose transformed BASH model from the previous processing step as reference instead. All vertices of the mesh $\mathcal{V}$ serve as reference points to determine the current pose in correspondence to the template mesh $\tilde{\mathcal{V}}$ which requires an identical geometric topology of all meshes in the SCAPE space. The rigid registration of two corresponding body parts $\tilde{B}$ with $N_{\tilde{B}}$ vertices is described as minimization of the root mean square error (RMSE):

$$\min_{\mathbf{R}_{\tilde{B}}} \sqrt{\frac{1}{N_{\tilde{B}}} \sum_{i=0}^{N_{\tilde{B}}-1} \|\mathbf{R}_{\tilde{B}} \cdot \tilde{\vec{v}}_i - \vec{v}_i\|^2}, \tag{2}$$

where $\tilde{\vec{v}}$ and $\vec{v}$ are the vertices of the SCAPE template mesh and the pose transformed BASH model, respectively. This optimization is solved as constrained Procrustes problem (Schönemann, 1966) using the Kabsch algorithm (Kabsch, 1976) and performing singular value decomposition (Golub and Reinsch, 1970). The obtained optimal rotations, i.e. the nearest orthogonal matrices, describe the rigid part transformations $\mathbf{R}_{\tilde{B}}$ of the SCAPE model.

The main feature of SCAPE is a realistic soft tissue deformation which is achieved by pose-induced transformations $\tilde{\mathbf{Q}}_f$ affecting the shape of each face f on the mesh based on training data and the current pose defined by $\mathbf{R}_{\tilde{B}}$. The rotations of adjacent joints $\tilde{J}_0, \tilde{J}_1$ and the learned regression vector $\tilde{\vec{a}}_{f,i,j} = (\tilde{a}_0, \tilde{a}_1, \tilde{a}_2, \tilde{a}_3, \tilde{a}_4, \tilde{a}_5, \tilde{a}_6)^T$ from the SCAPE framework are used to build the matrix:

$$\tilde{\mathbf{Q}}_f[i,j] = \left(\vec{\Delta}^T_{\mathbf{R}_{\tilde{J}_0}}, \vec{\Delta}^T_{\mathbf{R}_{\tilde{J}_1}}, 1\right)^T \cdot \tilde{\vec{a}}_{i,j,f}, \tag{3}$$

where i and j are the row and column indices, respectively. $\vec{\Delta}_{\mathbf{R}_{\tilde{J}}} = (\Delta_x, \Delta_y, \Delta_z)^T$ denotes the twist vector in angle-axis representation (Ma et al., 2004) of a joint rotation $\mathbf{R}_{\tilde{J}} = \mathbf{R}_{\tilde{B}_0} \cdot \mathbf{R}^T_{\tilde{B}_1}$ composed of adjacent rigid body parts $\tilde{B}_0$ and $\tilde{B}_1$. The body shape is omitted within this paper. Hence, the average shape of the trained SCAPE template mesh is used by setting shape deformation matrix $\tilde{\mathbf{D}}_f$ to the identity matrix for all faces.

The geometry of the new mesh is retrieved by minimizing the following non-linear optimization problem to avoid inconsistencies within the mesh instead of applying the rigid part rotations $\mathbf{R}_{\tilde{B}_f}$, pose dependent deformations $\tilde{\mathbf{Q}}_f$, and shape dependent deformations $\tilde{\mathbf{D}}_f$ directly to the vertices $\vec{v}$:

$$\min_{\vec{v}} \sum_{f=0}^{N_f-1} \sum_{i=1,2} \|\mathbf{R}_{\tilde{B}_f} \cdot \tilde{\mathbf{D}}_f \cdot \tilde{\mathbf{Q}}_f \cdot \tilde{\vec{v}}_{f,i} - (\vec{v}_{f,0} - \vec{v}_{f,i})\|^2. \tag{4}$$

The two edges $\vec{v}_{f,0} - \vec{v}_{f,i}$ with $i = 1,2$ span the face f built of the three vertices $\vec{v}_{f,0}$, $\vec{v}_{f,1}$, and $\vec{v}_{f,2}$.

Since the SCAPE framework omits the global position and orientation of the model in space for computational reasons, it has to be restored. A constrained orthogonal Procrustes problem is solved globally to register the SCAPE transformed mesh with the pose transformed mesh.

6 VISUALIZATION OF MUSCLE ACTIVITY

In addition to the animation of the model, muscle activation is visualized on the model's surface. The area of influence and the intensity are computed dynamically during run-time for the current time frame t.

6.1 Area of Influence

In the musculoskeletal model, a muscle $\hat{F}$ is characterized by a MTU with the 2D pathway $\hat{E}_{\hat{F}}(t)$. The 3D locations of the connected line segments are defined by multiple points $\hat{\vec{p}}$ fixed to the articulated skeleton. Before visualizing the muscle activity, a mapping from the 2D muscle pathways to the surface of the animated BASH model is established by finding the smallest distance from an underlying MTU to the model's surface. The perpendicular distance d is the shortest way from the line segment defined by $\hat{\vec{p}}_i$ and $\hat{\vec{p}}_{i+1}$ to a vertex. Vertices with a distance d smaller than a threshold $C_{maxDist}$ are included into the area of influence of the particular muscle.

6.2 Intensity Visualization

The identified areas of influence are used to highlight the muscle activation $\hat{a}_{\hat{F}}(t)$ on the surface via color coding. The force of the muscle contraction scales linearly with the muscle activation and the maximum isometric force $\hat{f}_{max_{\hat{F}}}$ (Thelen, 2003). Hence, the measure $i_{\hat{F}}(t)$ is composed as follows:

$$i_{\hat{F}}(t) = \frac{1}{C_{maxMeasure}} \cdot \hat{a}_{\hat{F}}(t) \cdot \hat{f}_{max_{\hat{F}}}. \tag{5}$$

The constant $C_{maxMeasure}$ is introduced to normalize by the maximum possible value that concentrates on a point. This enables an objective comparison of movement visualizations of distinct subjects with different

muscular constitutions. For each vertex, the measures $i_{\hat{F}}(t)$ of all influencing muscles are accumulated and added to the red color channel of the mesh. Due to the implementation in the fragment shader, color values are interpolated across the faces resulting in smooth transitions at the boundaries and overlapping areas of the influencing muscle regions.

7 EXPERIMENTS AND ANALYSES

We conducted experiments and analyses to confirm the functionality of the visualization approach using a full-body musculoskeletal model (Nitschke et al., 2020). The comprehensive musculoskeletal structure included 20 joints, 92 MTUs in the lower body and 46 markers.

The scaling functionality and the initial pose matching were evaluated with ten male test subjects. The generic musculoskeletal model (Nitschke et al., 2020) was scaled using the OpenSim scaling tool (Delp et al., 2007) to match the marker data of static trials of nine subjects (Dorschky et al., 2019b) (subject A to I). Additionally, an already scaled musculoskeletal model was used as subject J (Nitschke et al., 2020). To evaluate the scaling, the height H of the scaled BASH model was determined as the distance between the smallest and greatest y-coordinate of the mesh in the initial pose. The height should correlate with the body height of the subject.

The pose transformation and animation of the BASH model was analysed for subject J with simulated kinematics of straight running and curved running with 50 time samples available in the OpenSim file format (Nitschke et al., 2020). The proposed surface visualization of the muscle activity was tested with corresponding simulated muscle activation patterns of the motions and compared to the line representation in the OpenSim environment.

8 RESULTS AND DISCUSSION

Figure 5 presents the final surface visualization in comparison to the visualization from OpenSim (Seth et al., 2018). In the following, the individual processing and transformation steps are discussed separately.

8.1 Scaling of Body Proportions

The scaling of body proportions is an essential step for a representative visualization. An incorrect model size would lead to incorrect postures and would influence the analysis. For example, the ground contact time (Mooses et al., 2018) or foot clearance (Begg et al., 2007) are of interest for biomechanical analyses of gait, but would be erroneous.

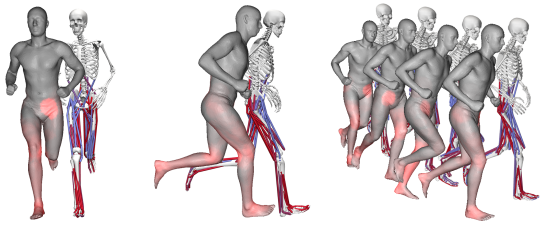

(a) (b) (c)

Figure 5: Final visualization of the kinematics including the muscle activation on the surface compared to the OpenSim (Seth et al., 2018) representation as reference. (a) and (b) show frontal and sagittal view of simulated straight running, respectively. (c) shows superimposed frames of simulated curved running.

Figure 6 shows the outcomes of the body part scaling for the ten subjects. The height H of the BASH model is greater than the actual body height for all subjects except for subject D and J. The mean and standard deviation of the absolute error is $6.7 \pm 4.8\,\mathrm{cm}$. Nevertheless, the proposed scaling is beneficial since the height of the scaled model is always closer to the body height than the generic model. We propose uniform scaling to produce robust result even when few markers are present. However, non-uniform scaling with individual scale factors for each dimension might be beneficial.

Nevertheless, the comparison of heights has to be interpreted with caution since marker placement or scaling of the musculoskeletal model can introduce errors as well. Furthermore, the estimated height H of the BASH model depends on the initial pose and might change when the model is transformed into SCAPE space. Also the skinning weights influence the shape and thus the scaling and height.

8.2 Initial Pose Matching

The quality of the mapping ${}^{\hat{J}}_{B}\mathbf{P}$ between the initial pose of the musculoskeletal model and the scaled BASH model influences the accuracy of the following pose transformations. Visual inspection shows that the BASH model is brought into a pose very similar to the pose of the musculoskeletal model (see Figure 7). However, the surface geometry does not completely envelope the musculoskeletal skeleton especially at the extremities due to missing marker data and missing mobility of hands and feet.

In inverse kinematics, the objective is to mini-

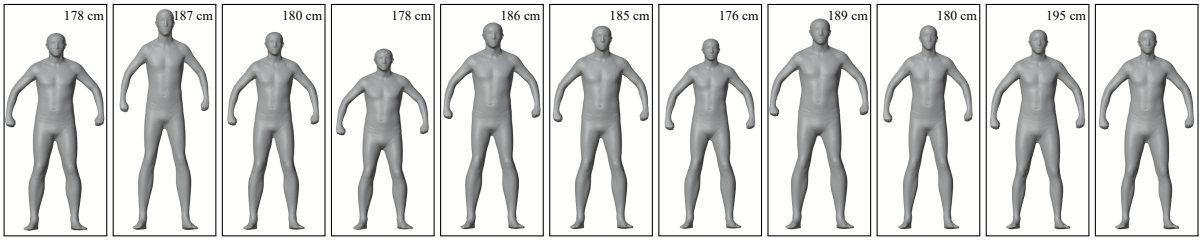

(a) Sub. A (b) Sub. B (c) Sub. C (d) Sub. D (e) Sub. E (f) Sub. F (g) Sub. G (h) Sub. H (i) Sub. I (j) Sub. J (k) Gen.

Figure 6: Frontal view of the scaled models before pose transformation and transformation into SCAPE space. Body heights reported by the subjects are displayed in the upper right corners. As reference, the generic model with a height H of 185 cm is displayed.

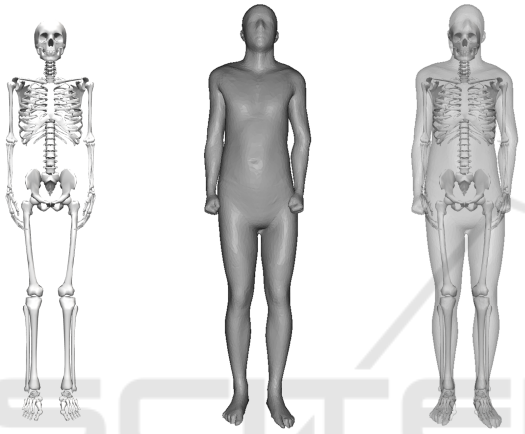

(a) (b) (c)

Figure 7: Visualization after the initial pose matching. (a), (b), and (c) show the skeletal representation of subject J in OpenSim (Seth et al., 2018), the proposed surface representation, and an overlay of both for comparison, respectively.

mize the marker tracking error. For the ten test subjects, the mean and standard deviation of the RMSE and of the maximum marker error is 2.1 ± 1.5 cm and 5.0 ± 3.0 cm, respectively. The error is therefore mainly within the range of the OpenSim recommendation (OpenSim, 2020). Similar to optical motion capture, the quality of the pose estimation highly depends on the marker placement.

8.3 Pose Transformation

The pose transformation is the main step of to animate the BASH model according to an input motion sequence. Due to the initial pose matching, kinematics are directly applied to the mesh using linear blend skinning which is commonly used in traditional computer animation. Although it produces accurate visualizations, some regions like elbow and hip are affected by strong deformations (see Figure 1).

8.4 Transformation into SCAPE Space

The transformation into SCAPE space makes use of a large training data set of full-body scans and thus can enrich the natural appearance of the animated human envelope. The SCAPE algorithm includes pose-induced deformations $\tilde{\mathbf{Q}}_f$ for realistic soft tissue deformation, e.g. muscle contractions, and shape dependent deformations $\tilde{\mathbf{D}}_f$ for realistic representation of the body structure.

The undesired strong deformations of the mesh at elbow and hip are reduced by the transformation into SCAPE space (see Figure 8a and 8b). Although the realism is enhanced, the accuracy of the surface representation suffers (see Figure 8c). Especially slight offsets at the feet might impact gait analysis where ground contact is crucial (Begg et al., 2007; Mooses et al., 2018).

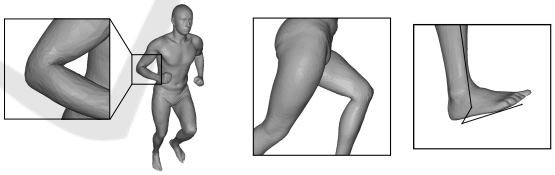

(a) (b) (c)

Figure 8: Views after transformation into SCAPE space for straight running. In (c) the articulated skeleton is overlaid.

The global registration of position and orientation after transformation into SCAPE space produces robust results due to the use of 12500 vertex correspondences. Alternatively, the pose transformation of the root bone could be used to apply the global position and orientation. Nevertheless, this would not acknowledge the fact that the SCAPE transformed model is fixed to the global coordinate system with a vertex at the right foot instead of the root bone.

We did not yet include shape dependent deformations by applying the shape coefficients provided by the SCAPE framework, which would enable a rep-

resentation of individual's anthropometry. For realism and identification with a virtual self, authenticity of a subject-related representation is key (Waltemate et al., 2018). Other statistical human models (Cheng et al., 2018) are more complex, but might also further increase the realism of the representation. Blending of strong deformations is improved (Hirshberg et al., 2012; Jain et al., 2010) and the *Skinned Multi Person Linear Model* (*SMPL*) (Loper et al., 2015) produced the most accurate results. *SMPL+H* (Romero et al., 2017), a recent extension of *SMPL*, allows posing and animation of individual fingers which would lead to an overall more natural representation. A slightly different aspect is included in the *Dyna* (Pons-Moll et al., 2015) model as it produces realistic dynamical soft tissue deformations during movement.

However, increased realism might not benefit the visualization. Lungrin et al. (2015) found that a nearly realistic human visualization evoke a strange feeling for an observer referred as the uncanny valley effect. Whether the visualization is perceived as realistic and whether subjects can identify themselves with the visualized model has to be confirmed in studies, especially with respect to the application and user group. In general, a balance between fidelity and degree of realism has to be found.

8.5 Visualization of Muscle Activity

MTUs are projected orthogonally onto the model surface to visualize muscle activity since it does not require additional data in contrast to other methods and allows therefore for easy visualization of various MTU sets. Furthermore, we hypothesize that a visualization on the surface is more accessible for non experts than volumetric muscle visualizations (Murai et al., 2010; Pronost et al., 2011; Van den Bogert et al., 2013) or line representations of OpenSim (Seth et al., 2018) or AnyBody (Damsgaard et al., 2006).

Depending on the application, the maximal distance $C_{maxDist}$ has to be chosen in order to represent the underlying MTUs well. For all figures in this paper, $C_{maxDist}$ is set to 8 cm as this produces appropriate results (see Figure 9). Alternatively, the maximum isometric force $\hat{f}_{max_{\hat{F}}}$ of each muscle could be included in the definition of the maximal distance since it is related to muscle volume.

Although the area is determined well for most muscles, it overflows into the other leg for the gracilis (see Figure 9c) and covers the complete shank instead of the rear part of the calf for the peroneus longus (see Figure 9d). This could be avoided by considering the orientation of the muscles with respect to the attached bones. Additionally, anatomical knowledge could be included, though this would limit the usability of the approach for other musculoskeletal models. Constraining the curvature in tangent space (Dennis et al., 1997) or using alternative algorithms like region growing (Adams and Bischof, 1994) could prevent propagation across valleys. Further improvements might be achieved by using barycentric coordinates (Rustamov, 2010) to overcome the limitation to vertex assignments.

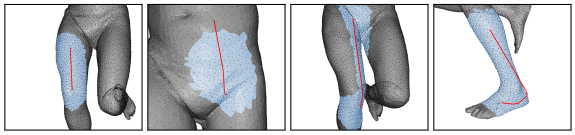

(a) vas_int_r (b) psoas_l (c) grac_r (d) per_long_l

Figure 9: Areas of influence (blue) assigned to the corresponding muscle pathways (red) using a maximal distance $C_{maxDist}$ of 8 cm.

For color coding of the determined area, the intensity is normalized with a constant $C_{maxMeasure} = 14\,000\,\text{N}$ to ensure comparability of the visualization across different motion sequences or subjects. Intensity normalization is for example important when evaluating temporal progress of diseases, gait training, or running technique of athletes or when comparing body constitutions or designs of equipment. The constant $C_{maxMeasure}$ should be chosen specific to the musculoskeletal model and application. Since the intensity measure $i_{\hat{F}}$ is added to the red color channel, the value of the red color channel could exceed its limits for inappropriate constants and would be cropped.

The color coding of the muscle activation is visually compared to the line representation of OpenSim (Seth et al., 2018) (see Figure 1). The muscle activation is highlighted plausibly on the surface with smooth transitions at borders and overlapping regions due to the color interpolation of the fragment shader. In Figure 5, kinematics and muscle activation of straight and curved running are visualized. Especially for people with little biomechanical knowledge, the surface representation likely appears more vivid and realistic. At the same time, it does not require additional data and can easily be applied to different musculoskeletal models. Hence, the proposed visualization of the muscle activity might offer a useful alternative compared to the 2D line (Damsgaard et al., 2006; Seth et al., 2018) or volumetric representation (Murai et al., 2010; Pronost et al., 2011; Van den Bogert et al., 2013).

9 CONCLUSION

We have presented a visualization pipeline to animate a skinned representation for biomechanical analysis of kinematics and muscle activity. The goal was to make biomechanical analysis more intuitive and realistic and increase accessibility for non-experts. To this end, we developed the BASH model to establish a bridge between the musculoskeletal model and a statistical surface model. Traditional animation character techniques and the SCAPE framework enabled body part scaling, pose transformations and realistic surface deformations for the input kinematics. Additionally, muscle activity related to the motion sequence is highlighted on the model's surface. Still, our approach does not require more input data than a traditional biomechanical approach: a musculoskeletal model, kinematic data and muscle activation. This ensures high usability and makes it easily applicable to other musculoskeletal models.

The proposed approach was evaluated using scaled musculoskeletal models of ten subjects (Dorschky et al., 2019b; Nitschke et al., 2020) and data of simulated straight and curved running (Nitschke et al., 2020). Our method achieved a realistic person-specific representation of the biomechanical input. Beside minor discrepancies, body part dimensions and the movement sequence was reflected accurately compared to state-of-the-art representations like OpenSim (Seth et al., 2018). The proposed 3D skinned human surface model seemed more accessible for non-experts, especially the visualization of muscular activity on the surface might offer an intuitive representation.

However, various topics could be investigated for further improvements. For applications where realtime feedback is required, such as gait retraining, *Realtime-SCAPE* (Chen et al., 2016) could be investigated. Furthermore, it might be possible to learn the pose regression parameters using the skeleton of the musculoskeletal model directly to eliminate some intermediate processing steps. The body shape parameters could be included to enhance person-specific visual representation. Besides expensive full-body scans or medical imaging, an extraction of shape coefficients from a photo of the subject could provide a practical solution (Bogo et al., 2016) to determine the body shape parameters. Constraint curvatures in tangent space (Dennis et al., 1997), region growing (Adams and Bischof, 1994), or barycentric coordinates (Rustamov, 2010), should be considered for the visualization of the muscle activity since they could be beneficial without requiring additional input data.

In this paper, the proposed methodology was evaluated by visual inspection and comparison with state-of-the-art tools. Since realism, intuitiveness and body ownership of a novel visualization cannot be measured objectively, there is a need to perform usability and perception studies for an application specific evaluation. Besides questionnaires and interviews about the proposed representation, efficiency of task execution should be studied with an user group.

The proposed pipeline is the first step to study usability and perception of biomechanical data visualization for non-experts. Our visualization method has the potential to enable non-experts, like patients, athletes and designers, to gain from biomechanical analysis for patient education, gait retraining, technique training, or design of equipment.

REFERENCES

Adams, R. and Bischof, L. (1994). Seeded Region Growing. *IEEE Transactions on Pattern Analysis and Machine Intelligence*, 16(6):641–647.

Anguelov, D., Srinivasan, P., Koller, D., Thrun, S., Rodgers, J., and Davis, J. (2005). SCAPE: Shape Completion and Animation of People. In *ACM Transactions on Graphics*, volume 24, pages 408–416.

Aubel, A. and Thalmann, D. (2001). Interactive modeling of the human musculature. In *Proceedings Computer Animation 2001. Fourteenth Conference on Computer Animation (Cat. No.01TH8596)*, pages 167–255.

Begg, R., Best, R., Dell'Oro, L., and Taylor, S. (2007). Minimum foot clearance during walking: Strategies for the minimisation of trip-related falls. *Gait and Posture*, 25(2):191–198.

Bencke, J., Aagaard, P., and Zebis, M. K. (2018). Muscle Activation During ACL Injury Risk Movements in Young Female Athletes: A Narrative Review. *Frontiers in Physiology*, 9(445):1–10.

Blemker, S. S. and Delp, S. L. (2005). Three-dimensional representation of complex muscle architectures and geometries. *Annals of Biomedical Engineering*, 33(5):661–673.

Bogo, F., Kanazawa, A., Lassner, C., Gehler, P., Romero, J., and Black, M. J. (2016). Keep it SMPL: Automatic estimation of 3D human pose and shape from a single image. In *European Conference on Computer Vision*, volume 9909 LNCS, pages 561–578. Springer.

Chen, Y., Cheng, Z. Q., Lai, C., Martin, R. R., and Dang, G. (2016). Realtime Reconstruction of an Animating Human Body from a Single Depth Camera. *IEEE Transactions on Visualization and Computer Graphics*, 22(8):2000–2011.

Cheng, Z. Q., Chen, Y., Martin, R. R., Wu, T., and Song, Z. (2018). Parametric modeling of 3D human body shape - A survey. *Computers and Graphics (Pergamon)*, 71:88–100.

Colaianni, M., Zollhoefer, M., Süßmuth, J., Seider, B., and Greiner, G. (2014). A Pose Invariant Statistical Shape

Model for Human Bodies. In *Proceedings of the 5th International Conference on 3D Body Scanning Technologies*, pages 327–336.

Damsgaard, M., Rasmussen, J., Christensen, S. T., Surma, E., and de Zee, M. (2006). Analysis of musculoskeletal systems in the AnyBody Modeling System. *Simulation Modelling Practice and Theory*, 14(8):1100–1111.

Delp, S. L., Anderson, F. C., Arnold, A. S., Loan, P., Habib, A., John, C. T., Guendelman, E., and Thelen, D. G. (2007). OpenSim: Open-source software to create and analyze dynamic simulations of movement. *IEEE Transactions on Biomedical Engineering*, 54(11):1940–1950.

Dennis, J., Maciel, M., Dennis, J., and El-Alem, M. (1997). A global convergence theory for general trust-region-based algorithms for equality constrained optimization. *SIAM Journal on Optimization*, 7(1):177–207.

Dorschky, E., Krüger, D., Kurfess, N., Schlarb, H., Wartzack, S., Eskofier, B. M., and van den Bogert, A. J. (2019a). Optimal control simulation predicts effects of midsole materials on energy cost of running. *Computer Methods in Biomechanics and Biomedical Engineering*, 22(8):869–879.

Dorschky, E., Nitschke, M., Seifer, A. K., van den Bogert, A. J., and Eskofier, B. M. (2019b). Estimation of gait kinematics and kinetics from inertial sensor data using optimal control of musculoskeletal models. *Journal of Biomechanics*, 95.

Ezati, M., Ghannadi, B., and McPhee, J. (2019). A review of simulation methods for human movement dynamics with emphasis on gait. *Multibody System Dynamics*, 47(3):265–292.

Falisse, A., Serrancolí, G., Dembia, C. L., Gillis, J., Jonkers, I., and De Groote, F. (2019). Rapid predictive simulations with complex musculoskeletal models suggest that diverse healthy and pathological human gaits can emerge from similar control strategies. *Journal of The Royal Society Interface*, 16(157):20190402.

Fey, N. P., Klute, G. K., and Neptune, R. R. (2012). Optimization of prosthetic foot stiffness to reduce metabolic cost and intact knee loading during below-knee amputee walking: A theoretical study. *Journal of Biomechanical Engineering*, 134(11):1–10.

Geijtenbeek, T. and Pronost, N. (2012). Interactive character animation using simulated physics: A state-of-the-art review. *Computer Graphics Forum*, 31(8):2492–2515.

Geijtenbeek, T., Steenbrink, F., Otten, B., and Even-Zohar, O. (2011). D-flow: immersive virtual reality and real-time feedback for rehabilitation. In *Proceedings of the 10th International Conference on Virtual Reality Continuum and Its Applications in Industry*, pages 201–208.

Golub, G. H. and Reinsch, C. (1970). Singular value decomposition and least squares solutions. In *Numerische Mathematik*, volume 14, pages 403–420. Springer.

Hasler, N., Stoll, C., Rosenhahn, B., Thormählen, T., and Seidel, H. P. (2009a). Estimating body shape of dressed humans. *Computers and Graphics (Pergamon)*, 33(3):211–216.

Hasler, N., Stoll, C., Sunkel, M., Rosenhahn, B., and Seidel, H. P. (2009b). A statistical model of human pose and body shape. *Computer Graphics Forum*, 28(2):337–346.

Hasler, N., Thormählen, T., Rosenhahn, B., and Seidel, H.-P. (2010). Learning skeletons for shape and pose. Number 212, pages 23–30.

Hirshberg, D. A., Loper, M., Rachlin, E., and Black, M. J. (2012). Coregistration: Simultaneous alignment and modeling of articulated 3D shape. *Lecture Notes in Computer Science (including subseries Lecture Notes in Artificial Intelligence and Lecture Notes in Bioinformatics)*, 7577 LNCS(PART 6):242–255.

Jain, A., Thormählen, T., Seidel, H. P., and Theobalt, C. (2010). MovieReshape: Tracking and Reshaping of Humans in Videos. *ACM Transactions on Graphics*, 29(6):1–10.

Jiang, Y., Van Wouwe, T., De Groote, F., and Liu, C. K. (2019). Synthesis of biologically realistic human motion using joint torque actuation. *ACM Transactions on Graphics (TOG)*, 38(4):1–12.

Kabsch, W. (1976). A solution for the best rotation to relate two sets of vectors. *Acta Crystallographica Section A*, 32(5):922–923.

Kavan, L., Collins, S., and O'Sullivan, C. (2009). Automatic linearization of nonlinear skinning. *Proceedings of I3D 2009: The 2009 ACM SIGGRAPH Symposium on Interactive 3D Graphics and Games*, pages 49–56.

Koelewijn, A. D. and van den Bogert, A. J. (2016). Joint contact forces can be reduced by improving joint moment symmetry in below-knee amputee gait simulations. *Gait and Posture*, 49:219–225.

Krüger, D. B. and Wartzack, S. (2015). Visualisation of biomechanical stress quantities within cad environments. In *Proceedings of the International Conference on Engineering Design, ICED*, pages 1–10.

Lee, D., Glueck, M., Khan, A., Fiume, E., Jackson, K., et al. (2012). Modeling and simulation of skeletal muscle for computer graphics: A survey. *Foundations and Trends® in Computer Graphics and Vision*, 7(4):229–276.

Lee, S. H., Sifakis, E., and Terzopoulos, D. (2009). Comprehensive biomechanical modeling and simulation of the upper body. *ACM Transactions on Graphics*, 28(4):1–17.

Lin, Y.-C. and Pandy, M. G. (2017). Three-dimensional data-tracking dynamic optimization simulations of human locomotion generated by direct collocation. *Journal of Biomechanics*, 59:1–8.

Loper, M., Mahmood, N., Romero, J., Pons-Moll, G., and Black, M. J. (2015). SMPL: A skinned multi-person linear model. *ACM Transactions on Graphics*, 34(6).

Ma, Y., Soatto, S., Košecká, J., and Sastry, S. (2004). *An Invitation to 3D Vision*, volume 19.

Magnenat-Thalmann, N., Laperrire, R., and Thalmann, D. (1988). Joint-dependent local deformations for hand animation and object grasping. In *In Proceedings on Graphics interface'88*. Citeseer.

Maurice, X., Sandholm, A., Pronost, N., Boulic, R., and Thalmann, D. (2009). A subject-specific software solution for the modeling and the visualization of muscles deformations. *Visual Computer*, 25(9):835–842.

McGuan, S. P. (2001). Human modeling–from bubblemen to skeletons. Technical report, SAE Technical Paper.

McLaughlin, T., Cutler, L., and Coleman, D. (2011). Character rigging, deformations, and simulations in film and game production. *ACM SIGGRAPH 2011 Courses, SIGGRAPH'11*.

Mooses, M., Haile, D. W., Ojiambo, R., Sang, M., Kerli, M., Lane, A. R., and Hackney, A. C. (2018). Shorter ground contact time and better running economy: Evidence from female kenyan runners. *Journal of Strength and Conditioning Research*.

Murai, A., Kurosaki, K., Yamane, K., and Nakamura, Y. (2010). Musculoskeletal-see-through mirror : Computational modeling and algorithm for whole-body muscle activity visualization in real time. *Progress in Biophysics and Molecular Biology*, 103(2-3):310–317.

Murai, A., Youn Hong, Q., Yamane, K., and Hodgins, J. K. (2017). Dynamic skin deformation simulation using musculoskeletal model and soft tissue dynamics. *Computational Visual Media*, 3(1):49–60.

Nitschke, M., Dorschky, E., Heinrich, D., Schlarb, H., Eskofier, B. M., Koelewijn, A. D., and Van den Bogert, A. J. (2020). Efficient trajectory optimization for curved running using a 3D musculoskeletal model with implicit dynamics. *Scientific Reports*, 10(17655).

OpenSim (2020). Getting started with inverse kinematics. Accessed on 03.05.2020.

Peeters, P. and Pronost, N. (2014). A practical framework for generating volumetric meshes of subject-specific soft tissue. *Visual Computer*, 30(2):127–137.

Pons-Moll, G., Romero, J., Mahmood, N., and Black, M. J. (2015). Dyna: A model of dynamic human shape in motion. *ACM Transactions on Graphics*, 34(4):1–14.

Pronost, N., Sandholm, A., and Thalmann, D. (2011). A visualization framework for the analysis of neuromuscular simulations. *Visual Computer*, 27(2):109–119.

Richards, R., van der Esch, M., van den Noort, J. C., and Harlaar, J. (2018). The learning process of gait retraining using real-time feedback in patients with medial knee osteoarthritis. *Gait & Posture*, 62:1–6.

Romero, J., Tzionas, D., and Black, M. J. (2017). Embodied hands: Modeling and capturing hands and bodies together. *ACM Transactions on Graphics*, 36(6).

Rustamov, R. M. (2010). Barycentric coordinates on surfaces. In *Computer Graphics Forum*, volume 29, pages 1507–1516. Wiley Online Library.

Schönemann, P. H. (1966). A generalized solution of the orthogonal procrustes problem.

Seth, A., Hicks, J. L., Uchida, T. K., Habib, A., Dembia, C. L., Dunne, J. J., Ong, C. F., DeMers, M. S., Rajagopal, A., Millard, M., et al. (2018). OpenSim: Simulating musculoskeletal dynamics and neuromuscular control to study human and animal movement. *PLoS Computational Biology*, 14(7):1–20.

Sueda, S., Kaufman, A., and Pai, D. K. (2008). Musculotendon simulation for hand animation. *ACM Transactions on Graphics*, 27(3).

Teran, J., Blemker, S., Hing, V., and Fedkiw, R. (2003). Finite volume methods for the simulation of skeletal muscle. pages 68–74. Eurographics Association.

Teran, J., Sifakis, E., Blemker, S. S., Ng-Thow-Hing, V., Lau, C., and Fedkiw, R. (2005). Creating and simulating skeletal muscle from the visible human data set. *IEEE Transactions on Visualization and Computer Graphics*, 11(3):317–328.

Thelen, D. G. (2003). Adjustment of muscle mechanics model parameters to simulate dynamic contractions in older adults. *Journal of Biomechanical Engineering*, 125(1):70–77.

Udow, S. J., Hobson, D. E., Kleiner, G., Masellis, M., Fox, S. H., Lang, A. E., and Marras, C. (2018). Educational needs and considerations for a visual educational tool to discuss parkinson's disease. *Movement Disorders Clinical Practice*, 5(1):66–74.

Van den Bogert, A. J., Geijtenbeek, T., Even-Zohar, O., Steenbrink, F., and Hardin, E. C. (2013). A real-time system for biomechanical analysis of human movement and muscle function. *Medical and Biological Engineering and Computing*, 51(10):1069–1077.

Van den Noort, J. C., Steenbrink, F., Roeles, S., and Harlaar, J. (2015). Real-time visual feedback for gait retraining: toward application in knee osteoarthritis. *Medical & Biological Engineering & Computing*, 53(3):275–286.

Vannatta, C. N. and Kernozek, T. W. (2015). Patellofemoral Joint Stress during Running with Alterations in Foot Strike Pattern. *Medicine & Science in Sports & Exercise*, 47(5):1001–1008.

Waltemate, T., Gall, D., Roth, D., Botsch, M., and Latoschik, M. E. (2018). The impact of avatar personalization and immersion on virtual body ownership, presence, and emotional response. *IEEE Transactions on Visualization and Computer Graphics*, 24(4):1643–1652.

Yang, Y., Yu, Y., Zhou, Y., Du, S., Davis, J., and Yang, R. (2014). Semantic parametric reshaping of human body models. In *2014 2nd International Conference on 3D Vision*, volume 2, pages 41–48. IEEE.